



národní  
úložiště  
šedé  
literatury

## **CFD Simulation of a Sub-millimetre Rising Bubble in a Stagnant Liquid.**

Crha, Jakub  
2020

Dostupný z <http://www.nusl.cz/ntk/nusl-437954>

Dílo je chráněno podle autorského zákona č. 121/2000 Sb.

Tento dokument byl stažen z Národního úložiště šedé literatury (NUŠL).

Datum stažení: 29.05.2024

Další dokumenty můžete najít prostřednictvím vyhledávacího rozhraní [nusl.cz](http://www.nusl.cz) .

## CFD SIMULATION OF A SUB-MILLIMETER RISING BUBBLE IN A STAGNANT LIQUID

J. Crha<sup>1,2</sup>, O. Kašpar<sup>1</sup>, P. Basařová<sup>1</sup>

<sup>1</sup> Department of Chemical Engineering, Faculty of Chemical Engineering, University of Chemistry and Technology, Technická 3, 166 28 Prague 6, Czech Republic

<sup>2</sup> Institute of Chemical Process Fundamentals, Czech Academy of Sciences, Rozvojová 2, 165 02, Czech Republic

### Abstract

Hydrodynamics of the multiphase apparatus is strongly affected by fluids used in the process. One of the main quantities, which determine the hydrodynamic behaviour is the rising velocity of gaseous bubbles. This velocity can be determined easily in small scale apparatuses, but it can be much more challenging in industrial-scale devices. For that reason, mathematical modeling is used. COMSOL Multiphysics, finite element CFD solver, was used to describe the behaviour of the single bubble rising in aqueous solutions of ethanol and *n*-propanol. Aqueous solutions of low-carbon alcohols are extensively used in many multiphase chemical processes such as distillation, flotation and in multiphase reactors. Bubble velocities and shapes obtained from the simulation were compared to experimental and theoretical values. Two initial diameters of bubbles were used – 0.6 and 0.8 mm. Terminal velocities and shapes deformations obtained from COMSOL of 0.6 mm bubble were in an agreement with theoretical and experimental values.

**Keywords:** Level set, bubble, single

## 1 Introduction

Many processes in the chemical industry use the continuous contact of two or more phases and their examples are distillation, absorption, flotation and multiphase reactors [1]. The multiphase system can be established by adding a second phase - spraying liquid droplets into the gas flow or by bubbling gaseous phase through the bulk of the liquid. The knowledge of physico-chemical properties of both phases is crucial as it has a great impact on how the formed bubbles will behave [2].

Terminal velocities of bubbles rising in stagnant liquids can be determined both experimentally and theoretically. For a single bubble, the theoretical approach of determining its velocity is straightforward. A simple expression can be derived from a balance of forces acting upon a bubble in steady state:

$$U_b = \sqrt{\frac{4(\rho_l - \rho_g)gd}{3C_d\rho_l}} \quad (1)$$

where  $U_b$  is a terminal velocity of the bubble in m/s,  $\rho$  is density in kg/m<sup>3</sup>, indexes *l* and *g* denote liquid and gaseous phase respectively,  $g$  is a gravitational acceleration in m/s<sup>2</sup> and  $C_d$  is drag coefficient of the bubble, which can be expressed differently according to the flow conditions. For spherical bubbles, the Mei approximation is often recommended [3]. For deformed bubbles an expression introduced by Rastello [4] is used:

$$C_{d,Mei} = \frac{16}{Re} \left\{ 1 + \left[ \frac{8}{Re} + \frac{1}{2}(1 + 3.315Re^{-0.5}) \right]^{-1} \right\} \quad (2)$$

$$C_{D,Rastello} = \frac{16}{Re} \left\{ \frac{1 + \frac{8}{15}(\kappa - 1) + 0.015(3G(\kappa) - 2)Re}{1 + 0.015Re} + \left[ \frac{8}{Re} + \frac{1}{2} \left( 1 + \frac{3.315H(\kappa)G(\kappa)}{Re^{1/2}} \right) \right]^{-1} \right\} \quad (3)$$

where  $G$  and  $H$  are polynomial functions of bubble aspect ratio  $\kappa$ , which defines the rate of bubble non-sphericity and can be determined as a ratio of the semi-major axis to the semi-minor axis in ellipse. A

detailed description of  $G(\kappa)$  and  $H(\kappa)$  can be found in [4]. The aspect ratio  $\kappa$  is often approximated [5] as a function of the Weber number:

$$We = \frac{\rho_l u_t^2 D_b}{\sigma} \quad (4)$$

$$\kappa = 1 + \frac{9}{64} We + \frac{3}{250} We^2 \quad (5)$$

These expressions cannot be used for calculating velocities of individual bubbles rising in apparatuses where bubbles are rising in swarms, as the bubbles are affecting each other and the bubble acceleration should be also considered [6].

With the advancement of computational power, another approach has emerged, which is a Computational Fluid Dynamics (CFD) modeling. CFD allows to simulate many different phenomena, but the model must be verified using independent experimental data. The main advantage of CFD modeling is that the knowledge collected from simplified simulation can be transferred to more complex simulations and results from such a model can be considered trustworthy.

Effectiveness of CFD solvers was proved in many studies dealing with single rising bubbles or droplets. Studies differ in the used solver (commercial or in-house), in the method used for tracking the interface and in physico-chemical properties of studied fluids. Eiswirth et al. [7] studied the behaviour of a toluene droplet of different diameters rising through the aqueous phase using the level set method in COMSOL Multiphysics. Klostermann et al. [8] demonstrated the capabilities of the Volume of Fluid method (VOF) in his study. Yujie et al. [9] studied the formation of air bubbles on orifice in the 2D domain with the VOF method in commercial solver Ansys Fluent. Other studies were done in open source solvers – Tripathi et al. [10] used Gerris solver to study dynamics of the initially spherical bubble, Hysing [11] used a rising bubble case for benchmarking different commercial CFD solvers to his code TP2D.

Above mentioned studies dealt mostly with air bubbles, which diameter is greater than 1 mm. In real apparatuses, even smaller bubbles appear. For that reason, a 2D axi-symmetric model of a sub-millimeter single rising bubble was created using COMSOL Multiphysics 5.3. The aim of this work was to compare terminal velocities obtained from CFD solver with theoretical and experimental values. The knowledge gained from this work will be used for modeling more complex phenomena such as more bubbles rising, the study of bubble surface mobility and interactions of bubbles.

## 2 Methods

The model of a single rising bubble was created in a COMSOL Multiphysics 5.3 using the built-in module Two-phase flow – Level set coupled with Laminar flow interface. For the fluid flow, the incompressible Navier-Stokes with continuity equation were used:

$$\rho \left( \frac{\partial \mathbf{u}}{\partial t} + \mathbf{u} \cdot \nabla \mathbf{u} \right) = \nabla \cdot [-p\mathbf{I} + \mu(\nabla \mathbf{u} + (\nabla \mathbf{u})^T)] + \mathbf{F} \quad (6)$$

$$\rho \nabla \cdot (\mathbf{u}) = 0 \quad (7)$$

here  $\rho$  is the fluid density, velocity vector,  $t$  is time,  $p$  is pressure,  $\mu$  is dynamic viscosity of the fluid and  $\mathbf{F}$  are external forces applied to the fluid. No turbulence model was used, as the laminar flow was considered due to the size of the bubbles and their expected velocity.

For the tracking of the two phase interface, COMSOL has three built-in methods – Level set, Phase field, and Moving mesh. Moving mesh method offers the highest resolution of the interface, but it is most computational power demanding. Another disadvantage is that this method cannot model topology changes, which can happen when the bubble bursts. Phase field method also offers high resolution of the interface, but it is also computational demanding, as it needs to solve two transport equations. The level set method only needs to solve one transport equation, therefore it is less computational power demanding [12]. Its capabilities were proved in many studies of two phase problems [7], [13]–[17]. These are the main reasons, why Level set method was chosen.

This interface tracking method was first introduced by S. Osher and J. Sethian [18]. In this method, the interface is represented by a zero contour of the level set function  $\Phi$ , which is defined as a signed distance function:

$$|\Phi(\vec{x})| = d(\vec{x}) = \min_{x_I \in I} (|\vec{x} - \vec{x}_I|) \quad (8)$$

where  $I$  denotes the interface,  $\Phi$  acquires values  $> 0$  on one side of the interface and  $\Phi < 0$  is on the other side. One disadvantage of this method is that the level set function needs a reinitialization step to preserve  $\Phi$  as a distance function, which is not conservative, thus numerical diffusion will occur [19]. Mass

conservation can be enhanced by using higher resolution of the computational mesh, which extends the computational time. Therefore, it is better to use conservative level set method, which COMSOL offers [12].

Liquid and gaseous phases largely differ in their values of density and viscosity. This causes large discontinuities across the interface, thus a smeared Heaviside function is introduced:

$$H(\Phi) = \begin{cases} 0 & \text{for } \Phi < -\varepsilon \\ \frac{1}{2} + \frac{\Phi}{2\varepsilon} + \frac{1}{2\pi} \sin\left(\frac{\pi\Phi}{\varepsilon}\right) & \text{for } -\varepsilon \leq \Phi \leq \varepsilon \\ 1 & \text{for } \Phi > \varepsilon \end{cases} \quad (9)$$

where the  $\varepsilon$  is a parameter controlling the thickness of the interface. In this form, the level set function acquires values from 0 – 1 and the interface is represented by the value 0.5 of the level set function [7]. The transport equation of the level set function can be written in this form:

$$\frac{\partial \Phi}{\partial t} + \nabla \cdot (\mathbf{u}\Phi) = \gamma \nabla \cdot \left( \varepsilon \nabla \Phi - \Phi(1 - \Phi) \frac{\nabla \Phi}{|\nabla \Phi|} \right) \quad (10)$$

where  $\gamma$  is the reinitialization parameter and its value is recommended as the highest velocity, which can occur in the domain. Eq. 10 is the Level set transport equation in its conservative form, which helps to maintain mass conservation during the simulation. Density and viscosity can be written in the terms of level set function:

$$\rho = \rho_1 + (\rho_2 - \rho_1)\Phi \quad (11)$$

$$\mu = \mu_1 + (\mu_2 - \mu_1)\Phi \quad (12)$$

in this case, index 1 corresponds to the domain where the level set function acquires value of  $< 0.5$  and index 2 is for the region where the function is  $> 0.5$ . One of the external forces applied to the bubble is surface tension. The Continuous surface force (CSF) [20] model is used for modeling surface tension effects.

The geometry was created in COMSOL as a 2D axi-symmetrical domain. This setup was chosen, as the studied bubble diameters were small (below 1 mm), thus steady rectilinear rise and fore- and aft-symmetry can be assumed [21]. Another advantage of the axi-symmetrical domain is, that it saves computational time, as it suffices to model only one half of the domain. The final dimensions of the domain were chosen as 6 mm in width and 40 mm in height. Chosen dimensions were the result of the width- and height- study of terminal velocity dependency on domain dimensions. On the walls and bottom of the domain a no-slip condition was imposed. In the middle, a symmetry condition and at the top a pressure outlet condition were used.

A free triangular mesh was used with uniform distribution. At first, mesh resolution dependency on terminal velocity was studied. From the study an ideal size of the elements was chosen – 0.05 and 0.1 mm for the 0.6- and 0.8-mm bubble, respectively. Both studies led to a final setup, which was used to calculate terminal velocities of bubbles rising in aqueous solutions of *n*-propanol, ethanol and pure water. For initializing the simulation, a MUMPS solver was used. PARDISO was used as a time dependent solver with Generalized alpha time stepping scheme.

### 3 Experiment

Terminal velocities of bubbles were determined experimentally from an the image sequences captured by a high-speed camera. The experimental apparatus consists of these parts: high-speed camera Photron SA1.1 with Navitar lense, cold light source, pressurized air inlet, single bubble generator and a glass column, which dimensions are 300x80x60 mm. Detailed description and a scheme of this apparatus can be found in [22].

The pressurized air flows through a valve into the air chamber beneath the column. Time of the chamber filling can be controlled, which determines the bubble diameter created at the capillary with the inner diameter 10  $\mu\text{m}$ . The bubble detachment is controlled by a quick pull down of the capillary. After the detachment, the high-speed camera records the bubble rise at a sufficient distance from the capillary where the movement of the bubble is straight and even.

A monochromatic image sequence of the bubble is obtained, which needs to be processed with image analysis software. In this work, the NIS-Elements software was used. After binarization of each image in the sequence, the time dependent parameters are obtained – x,y coordinates of the bubble centre, bubble equivalent diameter, area of the bubble and aspect ratio of the bubble  $\kappa$ , which and is defined as a ratio of semi-major axis to semi-minor axis in an ellipse (see Figure 1). This parameter defines the rate of bubble shape deformation. For a spherical bubble  $\kappa$  is equal to 1.

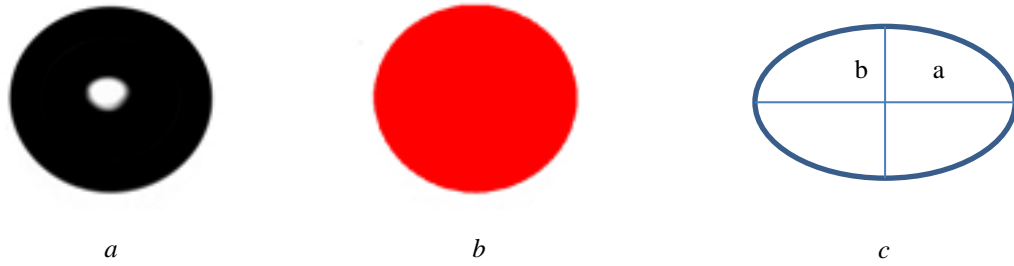


Figure 1: a) Monochromatic image of the bubble b) Binarized image of the bubble c) Aspect ratio

The experiment was conducted for bubbles rising in aqueous solutions of *n*-propanol, ethanol and pure water. Physico-chemical properties (density, surface tension and dynamic viscosity) of each solution were measured at a temperature 24 °C. Details, used techniques and instruments can be found in [22].

Molar fraction [-]	Density [kg/m <sup>3</sup> ]	Surface tension [mN/m]	Dynamic viscosity [mPa.s]
<b>Ethanol</b>			
0.1	962.7	36.6	1.97
0.2	934.2	29.9	2.31
0.3	904.8	27.9	2.34
0.5	858.3	24.9	1.94
0.8	810.3	23.0	1.39
1	785.6	21.8	1.10
<b>Propanol</b>			
0.1	953.8	26.2	2.20
0.2	914.2	25.3	2.61
0.3	887.5	25.4	2.82
0.5	850.9	24.9	2.60
0.8	816.8	24.1	2.20
1	799.9	23.3	2.04
<b>Water</b>			
1	997.1	72.2	0.89

Table 1: Values of physico-chemical properties of ethanol, *n*-propanol, their aqueous solutions, and water

## 4 Results

From each bubble sequence, an averaged terminal velocity and shape deformation value (aspect ratio of the bubble) were obtained. Experimental values were used for CFD model validation and compared to the theoretical velocities and shapes. Experimental velocities were not measured for 0.8 mm bubble in solutions of ethanol and propanol, as the capillary size in experimental apparatus was not suitable for creating larger bubbles. The values of the bubble terminal velocity in COMSOL was obtained by using this expression, which can be found in [16]:

$$u_t = \frac{\int_{\Omega_1} v \, d\Omega}{\int_{\Omega_1} d\Omega} \quad (13)$$

where  $v$  is the vertical component of the velocity field,  $\Omega$  is the domain and index  $l$  is the part of the domain where the bubble is. Bubble reached a steady state velocity after 0.05 seconds. The average computational time for 0.8 mm bubble rising for 0.2 s was 9 hours. In the case of 0.6 mm bubble the computational time was around 12 hour, as it was computed on finer mesh. In the Table 2, the calculated value of terminal velocity is denoted as  $U_{\text{Comsol}}$ . Similarly, the bubble aspect ratio is described as  $\kappa_{\text{Comsol}}$ .

Theoretical velocity was computed using Eq. 1 with two different expressions for the drag coefficient. An expression (Eq. 2) proposed by Mei [3] for spherical bubbles, and for deformed bubbles an expression introduced by Rastello (Eq.3) [4] were used. In Table 2, these velocities are denoted as  $U_{Mei}$  and  $U_{Rastello}$ , respectively. Obtained velocities for the bubble having 0.6 mm diameter from COMSOL simulations are in a very good agreement both with the theoretical and experimental values throughout the whole concentration range of ethanol and propanol. The largest error is around 10 % when compared to experimental velocities for both cases. It should be emphasized here that as the concentration of alcohol in the solution increases, the density decreases and at the same time the viscosity changes (the maximum is around 30 mol. %, see Table 1) and therefore the resulting bubble velocities differ.

Simulations in COMSOL reflected the change in the physical properties of the liquid perfectly. Velocities obtained for the bubble with diameter 0.8 mm were compared only to theoretically calculated velocities using the expression for spherical bubbles ( $U_{Mei}$ ) and for slightly deformed bubbles ( $U_{Rastello}$ ). It should be concluded from this comparison that the Rastello relation for the drag coefficients (Eq. 3) is more suitable. For smaller bubbles ( $D_b = 0.6$  mm), the bubble aspect ratio reaches a maximum of 1.03. The experimental values and the values calculated using the Weber number (Eq. 5) do not differ. Aspect ratio values from the simulation are slightly higher, and therefore the terminal bubble velocity values are lower. In the case of larger bubbles, this effect is more important. The bubble aspect ratio ranges from 1.04 to 1.15, with the simulation values always higher than the Weber number calculation. The greatest error is around 12 % in the case of bubble in water.

molar fraction	water	ethanol						<i>n</i> -propanol					
		0.1	0.2	0.3	0.5	0.8	1	0.1	0.2	0.3	0.5	0.8	1
$D_b = 0.6$ mm, terminal bubble velocity (mm/s)													
$U_{COMSOL}$	150	82	75	73	78	89	99	77	69	66	67	71	73
$U_{exp}$	142	73	70	67	73	85	-	71	62	59	61	65	67
$U_{Mei}$	141	78	69	67	73	88	101	72	63	59	60	65	68
$U_{Rastello}$	139	78	69	67	73	87	99	72	62	58	60	65	67
$D_b = 0.8$ mm, terminal bubble velocity (mm/s)													
$U_{COMSOL}$	189	114	102	99	106	123	135	105	94	89	91	97	100
$U_{Mei}$	231	122	107	103	113	138	161	112	97	90	92	100	104
$U_{Rastello}$	214	118	104	101	110	131	146	108	95	88	91	98	102
$D_b = 0.6$ mm, bubble aspect ratio $\kappa$													
$\kappa_{COMSOL}$	1.05	1.02	1.01	1.02	1.03	1.03	1.04	1.03	1.02	1.02	1.02	1.02	1.02
$\kappa_{exp}$	1.03	1.02	1.01	1.02	1.02	1.02	-	1.01	1.01	1.01	1.01	1.01	1.01
$\kappa_{Weber}$	1.03	1.02	1.01	1.01	1.02	1.02	1.03	1.02	1.02	1.01	1.01	1.01	1.02
$D_b = 0.8$ mm, bubble aspect ratio $\kappa$													
$\kappa_{COMSOL}$	1.12	1.06	1.06	1.06	1.07	1.11	1.15	1.07	1.06	1.05	1.05	1.06	1.06
$\kappa_{Weber}$	1.07	1.04	1.05	1.04	1.05	1.07	1.09	1.05	1.04	1.03	1.03	1.04	1.04

Table 2: Resulting velocities and shape deformations of 0.6 and 0.8 mm bubbles in water and aqueous solutions of ethanol and propanol

## 5 Conclusions

In this work, the model of a single rising bubble was created using Level set method in CFD solver COMSOL Multiphysics. Obtained terminal velocities and values of aspect ratios of the 0.6 mm bubble perfectly agree with experimental values and theoretical velocities of spherical bubble. In the case of 0.8 mm bubble, experimental velocities were not available, thus simulation results were compared only to theoretical velocities. Aspect ratio values of the 0.8 mm bubble from COMSOL were higher than theory expected. In this case the bubble velocities is better to compare with velocities of slightly deformed bubbles, which give better agreement with simulation results. In this work was proved that Level set

method is suitable for simulations of two phase flow phenomena in pure liquids. COMSOL showed that it is capable of handling large differences in physico-chemical properties.

## Acknowledgement

This work was supported by a Czech Science Foundation (GACR) grant 19-09518S.

## References

- [1] Sommerfeld, M. and Horender, S., "Fluid Mechanics," *Ullmann's Encyclopedia of Industrial Chemistry*. 15-Oct-2012, doi: doi:10.1002/14356007.b01\_05.pub2.
- [2] Kulkarni, A. A. and Joshi, J. B., "Bubble formation and bubble rise velocity in gas-liquid systems: A review," *Ind. Eng. Chem. Res.*, vol. 44, no. 16, pp. 5873–5931, 2005, doi: 10.1021/ie049131p.
- [3] Mei, R., Klausner, J. F., and Lawrence, C. J., "A note on the history force on a spherical bubble at finite Reynolds number," *Phys. Fluids*, vol. 6, no. 1, pp. 418–420, 1994, doi: 10.1063/1.868039.
- [4] Rastello, M., Marié, J.-L., and Lance, M., "Drag and lift forces on clean spherical and ellipsoidal bubbles in a solid-body rotating flow," *J. Fluid Mech.*, vol. 8, no. 11, pp. 21062–21070, 2011, doi: 10.1017/jfm.2011.240.
- [5] Moore, D. W., "The velocity of rise of distorted gas bubbles in a liquid of small viscosity," *J. Fluid Mech.*, vol. 23, no. 04, p. 749, Dec. 1965, doi: 10.1017/S0022112065001660.
- [6] Smolianski, A., Haario, H., and Luukka, P., "Numerical study of dynamics of single bubbles and bubble swarms," *Appl. Math. Model.*, vol. 32, no. 5, pp. 641–659, May 2008, doi: 10.1016/J.APM.2007.01.004.
- [7] Eiswirth, R. T., Bart, H. J., Atmakidis, T., and Kenig, E. Y., "Experimental and numerical investigation of a free rising droplet," *Chem. Eng. Process. Process Intensif.*, vol. 50, no. 7, pp. 718–727, 2011, doi: 10.1016/j.cep.2011.04.008.
- [8] Klostermann, J., Schaake, K., and Schwarze, R., "Numerical simulation of a single rising bubble by VOF with surface compression," *Int. J. Numer. METHODS FLUIDS Int. J. Numer. Meth. Fluids*, 2012, doi: 10.1002/flid.3692.
- [9] Yujie, Z., Mingyan, L., Yonggui, X., and Can, T., "Two-dimensional volume of fluid simulation studies on single bubble formation and dynamics in bubble columns," *Chem. Eng. Sci.*, vol. 73, pp. 55–78, 2012, doi: 10.1016/j.ces.2012.01.012.
- [10] Tripathi, M. K., Sahu, K. C., and Govindarajan, R., "Dynamics of an initially spherical bubble rising in quiescent liquid," *Nat. Commun.*, vol. 6, pp. 1–9, 2015, doi: 10.1038/ncomms7268.
- [11] Hysing, S.-R., "Numerical Simulation of Immiscible Fluids with FEM Level Set Techniques," 2007.
- [12] COMSOL Multiphysics Reference Manual, *COMSOL Multiphysics Reference Manual, version 5.3*. 2017.
- [13] Grzybowski, H. and Mosdorf, R., "Modelling of two-phase flow in a minichannel using level-set method," *J. Phys. Conf. Ser.*, vol. 530, no. 1, 2014, doi: 10.1088/1742-6596/530/1/012049.
- [14] Olsson, E. and Kreiss, G., "A conservative level set method for two phase flow," *J. Comput. Phys.*, vol. 210, no. 1, pp. 225–246, 2005, doi: 10.1016/j.jcp.2006.12.027.
- [15] Balcázar, N., Lehmkuhl, O., Jofre, L., and Oliva, A., "Level-set simulations of buoyancy-driven motion of single and multiple bubbles," *Int. J. Heat Fluid Flow*, vol. 56, pp. 91–107, Dec. 2015, doi: 10.1016/J.IJHEATFLUIDFLOW.2015.07.004.
- [16] Hysing, S., "Mixed element FEM level set method for numerical simulation of immiscible fluids," *J. Comput. Phys.*, vol. 231, no. 6, pp. 2449–2465, 2012, doi: 10.1016/j.jcp.2011.11.035.

- 
- [17] Gollakota, A. R. K. and Kishore, N., “CFD study on rise and deformation characteristics of buoyancy-driven spheroid bubbles in stagnant Carreau model non-Newtonian fluids,” *Theor. Comput. Fluid Dyn.*, vol. 32, no. 1, pp. 35–46, 2018, doi: 10.1007/s00162-017-0436-y.
- [18] Osher, S. and Sethian, J. A., “Fronts propagating with curvature-dependent speed: Algorithms based on Hamilton-Jacobi formulations,” *J. Comput. Phys.*, vol. 79, no. 1, pp. 12–49, 1988, doi: 10.1016/0021-9991(88)90002-2.
- [19] Sethian, J. A. and Smereka, P., “Level Set Methods for fluid interfaces,” *Annu. Rev. Fluid Mech.*, vol. 35, no. 1, pp. 341–372, 2003, doi: 10.1146/annurev.fluid.35.101101.161105.
- [20] Brackbill, J. ., Kothe, D. ., and Zemach, C., “A continuum method for modeling surface tension,” *J. Comput. Phys.*, vol. 100, no. 2, pp. 335–354, Jun. 1992, doi: 10.1016/0021-9991(92)90240-Y.
- [21] Clift, R., Grace, J. R., and Weber, M. E., “Bubbles, drops, and particles .” Academic Press , New York , 1978.
- [22] Basařová, P., Pišlová, J., Mills, J., and Orvalho, S., “Influence of molecular structure of alcohol-water mixtures on bubble behaviour and bubble surface mobility,” *Chem. Eng. Sci.*, vol. 192, pp. 74–84, 2018, doi: 10.1016/j.ces.2018.07.008.